Published as: *Cell*. 2008 June 13; 133(6): 963–977.

The Amyotrophic Lateral Sclerosis 8 protein VAPB is cleaved, secreted, and acts as a ligand for Eph receptors

Hiroshi Tsuda[1], **Sung Min Han**[2], **Youfeng Yang**[2], **Chao Tong**[1], **Yong Qi Lin**[3], **Kriti Mohan**[1], **Claire Haueter**[3], **Anthony Zoghbi**[1], **Yadollah Harati**[4], **Justin Kwan**[4], **Michael A. Miller**[2], and **Hugo J. Bellen**[1,3,5,*]

1 *Department of Molecular and Human Genetics, Baylor College of Medicine, University of Alabama, Birmingham, Alabama*

2 *Department of Cell Biology, School of Medicine, University of Alabama, Birmingham, Alabama*

3 *Howard Hughes Medical Institute, Baylor College of Medicine, Houston, Texas 77030*

4 *Department of Neurology, Baylor College of Medicine, Houston, Texas 77030*

5 *Program in Developmental Biology, Baylor College of Medicine, Houston, Texas 77030*

Summary

VAP proteins (human VAPB/ALS8, *Drosophila* VAP33, and *C. elegans* VPR-1) are homologous proteins with an amino-terminal major sperm protein (MSP) domain and a transmembrane domain. The MSP domain is named for its similarity to *C. elegans* MSP protein, a sperm-derived hormone that binds to the Eph receptor and induces oocyte maturation. A point mutation (P56S) in the MSP domain of human VAPB is associated with Amyotrophic Lateral Sclerosis (ALS), but the mechanisms underlying the pathogenesis are poorly understood. Here we show that the MSP domains of VAP proteins are cleaved and secreted ligands for Eph receptors. The P58S mutation in VAP33 leads to a failure to secrete the MSP domain as well as ubiquitination, accumulation of inclusions in the endoplasmic reticulum, and an unfolded protein response. We propose that VAP MSP domains are secreted and act as diffusible hormones for Eph receptors. This work provides insight into mechanisms that may impact the pathogenesis of ALS.

Keywords

ALS; SMA; VAP33A; MSP; *Drosophila*; *C. elegans*; Eph receptors; ER inclusions; muscles; neurons

Introduction

The mechanisms that underlie Amyotrophic Lateral Sclerosis (ALS) are poorly understood. ALS is associated with the dysfunction or death of motor neurons in the motor cortex, brain stem, and spinal cord. About 10-15% of all ALS cases are familial, whereas 85%-90% are sporadic (Boillee et al., 2006; Bruijn et al., 2004). The most common form of familial ALS is

*Corresponding author: Hugo J. Bellen, Tel: 713-798-5272, Fax: 713-798-3694, email: hbellen@bcm.tmc.edu.

caused by mutations in superoxide dismutase 1 (SOD1). Recently, Nishimura et al. (2004) identified another gene that causes familial ALS, ALS8. This gene encodes the VAMP (Synaptobrevin) Associated Protein B (VAPB). Lesions in SOD1 and ALS8 have been shown to cause a wide variety of symptoms that typically include motor neuron death, but vary widely in the age of onset, the speed of progression, and the motor neuron populations that are affected. For example, a single amino acid change in ALS8 (P56S) causes typical ALS, atypical slowly progressive ALS, and spinomuscular atrophy (SMA) with an age of onset between 25 and 52 years and a speed of progression between 2 and 30 years (Nishimura et al., 2004). The cause of this variation may be due to genetic modifiers, partial redundancy, or environment.

VAPB is closely related to VAPA, which has been shown to associate with the cytoplasmic face of the endoplasmic reticulum (ER) and the Golgi apparatus (Kaiser et al., 2005; Skehel et al., 2000; Soussan et al., 1999). Human VAPB (hereafter named hVAP) protein is about 30 kDa and has homologues in *C. elegans* (VPR-1), *Drosophila* (DVAP33-A, hereafter named dVAP) (Pennetta et al., 2002) and numerous other species, including yeast (Scs2p) (Kagiwada and Zen, 2003). VAPs consist of an amino (N)-terminal domain of about 125 residues called the major sperm protein (MSP) domain, which is conserved among all VAP family members (Nishimura et al., 1999; Weir et al., 1998) (Figure 1A). The central region is predicted to form a coiled-coil motif. The hydrophobic carboxy (C)-terminus acts as a membrane anchor. The MSP domain is named for its similarity to nematode MSPs, the most abundant proteins in nematode sperm (Bottino et al., 2002). MSP and VAP MSP domains fold into evolutionarily conserved immunoglobulin-type seven-stranded beta sandwiches (Baker et al., 2002; Kaiser et al., 2005), suggesting a common function.

The main difference between VAPs and MSP is their proposed functions. *C. elegans* MSPs do not contain a coiled-coil motif or a transmembrane domain (Ward et al., 1988). MSPs have an intracellular cytoskeletal function, which depends on their ability to polymerize in the absence of actin or myosin (Bottino et al., 2002) and an extracellular signaling function during fertilization (Miller et al., 2001). MSP is secreted from the sperm cytosol into the reproductive tract by an unconventional process (Kosinski et al., 2005). Extracellular MSP directly binds to the VAB-1 Eph receptor and other yet to be identified receptors on oocyte and ovarian sheath cell surfaces (Corrigan et al., 2005; Govindan et al., 2006; Miller et al., 2003). MSP induces oocyte maturation, which prepares oocytes for fertilization and embryogenesis, and sheath contraction (Miller et al., 2001).

The Eph receptors are an evolutionarily conserved class of receptor tyrosine kinases that bind to membrane-attached ligands called ephrins (Palmer and Klein, 2003). Ephrins act in parallel to gap junctions to inhibit oocyte maturation, and MSP antagonizes this inhibitory circuit (Govindan et al., 2006; Miller et al., 2003; Whitten and Miller, 2007). MSP induces activation of the MAP kinase and Ca^{2+}/calmodulin-dependent protein kinase II cascades (Corrigan et al., 2005; Miller et al., 2001) as well as reorganization of the oocyte microtubule cytoskeleton (Harris et al., 2006).

The biological function of VAPs is not well understood. Yeast Scs2p is involved in phosphatidylinositol-4-phosphate synthesis and ceramide transport (Brickner and Walter, 2004; Kagiwada and Zen, 2003). VAPs have been reported to associate with the ER (Amarilio et al., 2005; Kaiser et al., 2005; Soussan et al., 1999). Overexpression of hVAP in human cells affects the structural integrity of the ER (Teuling et al., 2007) through interaction with Nir (N-terminal domain-interacting receptor) proteins (Amarilio et al., 2005). VAPs also interact with Oxysterol-binding protein (OSBP) and Ceramide transfer protein. These interactions are each mediated through FFAT (two phenylalanines in an acidic tract) domains (Amarilio et al., 2005; Kaiser et al., 2005; Loewen and Levine, 2005). Taken together, the results suggest that

VAPs might play a role in fatty acid metabolism (Perry and Ridgway, 2006; Wang et al., 2005).

To further define the role of VAPs, we have been characterizing *Drosophila* dVAP (Pennetta et al., 2002). dVAP modulates the number and size of neuromuscular junction (NMJ) boutons. Loss of dVAP disrupts the presynaptic microtubule architecture (Pennetta et al., 2002), causes an increase in miniature excitatory junctional potential (mEJP) size as well as an increase in postsynaptic glutamate receptor clustering (Chai et al., 2008).

Here, we present evidence that VAP MSP domains are secreted ligands for Eph receptors. We propose that secreted MSP domains function as trophic factors by binding to Eph receptors and other cell surface receptors. The P56S mutation that causes ALS8 (P58S in dVAP) induces insoluble aggregates that are ubiquitinated in flies. P58S also leads to an accumulation of mutant and wild type protein in the ER, an unfolded protein response (UPR), and a failure to secrete the MSP domain. Collectively, our results suggest that P56S affects a cell autonomous pathway involving the ER and UPR as well as a cell non-autonomous pathway involving Eph receptor signaling.

Results

The N-terminal portion of dVAP is secreted

We previously generated guinea pig polyclonal antibodies against dVAP which specifically detect the protein on Western blots (Pennetta et al., 2002). Although these antibodies (GP33 or GP36) detect overexpressed dVAP, the presence of some immunofluorescence signals in *dVAP* null mutant tissue ($dVAP^{\Delta 20}$ or $dVAP^{\Delta 488}$) suggests that they recognize a non-specific component (data not shown). We generated new antisera against dVAP (Rb92) and confirmed antibody specificity (Figure 1B and 1C). To assess the cellular dVAP distribution, we co-stained fly tissues with anti-dVAP and cellular markers. We find that dVAP is associated with the ER in wing imaginal disc cells (data not shown) and salivary gland cells (Figure S1A-C). dVAP is also localized to the cell membrane or just beneath the cell membrane based on its partial colocalization with Spectrin (Pesacreta et al., 1989) (Figure 1D-I). In addition, we observed numerous punctae (arrows in Figure 1H) in wild type tissue which neither colocalize with Spectrin or Boca, an ER marker (Figure 1I and data not shown). These punctae are most often found near cell boundaries, suggesting that they are in the extracellular space.

To determine if dVAP is present extracellularly, we used protocols for distinguishing between extracellular and intracellular antigens in wing discs (Seto and Bellen, 2006; Strigini and Cohen, 2000). Extracellular dVAP is found in wild type discs (Figure 2A), but is absent in *dVAP* null mutant discs (Figure 2B). These data indicate that a portion of dVAP or the whole protein can be secreted.

There are at least two possible alternatives. The wing cells reverse dVAP polarity such that it remains membrane-anchored but the N-terminus is extracellular. Alternatively, dVAP is cleaved intracellularly and a portion is secreted. To determine which portion of dVAP is extracellular, we generated transgenic flies carrying the *dVAP* cDNA tagged with an N-terminal FLAG tag and a C-terminal HA tag. This UAS construct is able to rescue the lethality associated with *dVAP* loss, indicating that it is functional (data not shown). To examine the localization of the tagged protein, we used the dpp-GAL4 driver (Figure 2C). Anti-FLAG antibody staining without membrane permeabilization shows that the N-terminal portion of dVAP is extracellular (Figure 2D and E), whereas staining with anti-HA antibody (Figure 2D and F) shows that the C-terminal portion is intracellular. We then incubated the live discs expressing FLAG-dVAP-HA protein with anti-FLAG antibody, fixed, permeabilized the cells, and incubated with anti-HA antibody. As shown in Figure 2 G-I, the N-terminal part of dVAP

is more broadly distributed than the C-terminal portion, typically extending from 1-3 cells beyond the dpp-GAL4 expressing cells, which indicates that the N-terminal portion is secreted and diffuses away. In summary, our data provide strong evidence that the dVAP protein is cleaved and that an N-terminal portion is secreted.

The MSP domain of dVAP is cleaved

Western blots should allow identification of the processed forms of the protein. We extracted proteins from larvae expressing FLAG-dVAP-HA and performed western blotting with anti-dVAP (GP33) and anti-FLAG. The size of the full length protein is about 33kDa. Extracts from wild type third instar larvae (Figure 2J, Canton S, CS, left) show a broad set of bands around 33 kDa as well as less abundant smaller sized bands. At least four different proteins (235aa, 238aa, and two different 269aa proteins, which all seem to differ in the coiled-coil domain) can be derived from the *dVAP* locus (FlyBase ID; FBgn0029687). These proteins migrate in the 28-33kDa range whereas the 17 kDa band is probably a cleavage product. None of these proteins is present in *dVAP* null mutants (data not shown).

To determine the cleavage profile of the overexpressed FLAG-dVAP-HA protein we probed the same blot for the N-terminal FLAG tag. We observe no staining in wild type controls (CS) and *dVAP* null mutant animals (not shown). However, we observe 22-37 kDa bands as well as multiple bands in the 13-18 kDa range (Figure 2J, bracket). Since we expressed a single isoform of FLAG-dVAP-HA (around 38kDa), many of the bands labeled with anti-FLAG must be cleavage products. Probing the blot with the HA tag confirms that the FLAG-containing products are uniquely N-terminal. The size of the N-terminal cleavage product indicates that it must contain most or all the MSP domain (about 125 amino acids). The bands revealed by anti-HA (10-15kD) correspond to multiple cleavage products. In summary, our data suggest that the MSP domain of the dVAP protein is cleaved from the transmembrane domain.

To determine if secretion of the MSP domain is observed in humans, we examined the expression of hVAP in flies, human leukocytes, and human serum. The anti-hVAP antibody was raised against the full length (30 kDa) human protein (Amarilio et al., 2005). This antibody does not crossreact with the *Drosophila* protein (Figure 2K, control, lane C155/+). When hVAP is expressed in flies, we detect full length protein and cleavage products. In human leukocytes, we detect the full length protein as well as additional 25 kDa and 18 kDa bands (Figure 2K, lane WBC). In contrast, we only detect the 18 kDa band in human serum (Figure 2K-L, lane Serum and Figure S1 D). Taken together, our data indicate that VAP MSP domains are secreted and suggest that the hVAP MSP domain is found in human serum.

P58S dVAP fails to be secreted, aggregates in the cytoplasm, and is ubiquitinated

In humans, the P56S mutation in *hVAP* causes ALS8 (Nishimura et al., 2004). To better understand the nature of the mutation, we generated a UAS-P58S dVAP construct which corresponds to the P56S mutation in hVAP. We examined the subcellular localization of P58S dVAP and wild type (WT) dVAP proteins expressed ectopically in the wing disc under the control of the dpp-GAL4 driver. As shown in Figure 3A and 3B, when the cells are not permeabilized we observe extracellular staining of WT dVAP. However, little or no extracellular staining is observed when P58S dVAP is overexpressed (Figure 3C and 3D). To further examine the effect of the mutation on secretion, we overexpressed the WT and P58S dVAP MSP domains in S2 cells. As shown in Figure S2A, WT dVAP MSP, but not mutant dVAP MSP, is present in the conditioned medium. These data indicate that the P58S mutation prevents secretion of the MSP domain.

The staining of permeabilized wing disc cells with anti-dVAP antibodies shows that the P58S mutation causes the dVAP protein to localize to intracellular aggregates (Figure 3E-H). These

aggregates resemble cytoplasmic protein inclusions found in ALS patients (Boillee et al., 2006; Bruijn et al., 2004). To compare the localization of WT and P58S in motor neurons, we expressed the transgenes under control of C155- and C164-GAL4 in a *dVAP* null mutant background. WT dVAP is present in the cytoplasm and axons (Figure 3I; Figure S2B-C and F-G), whereas P58S dVAP exhibits a very different profile with numerous cytoplasmic punctae (Figure 3K; Figure S2D-E) and axonal aggregates (Figure S2H-I).

To test whether P58S dVAP is ubiquitinated, we co-stained flies expressing WT or P58S dVAP with anti-dVAP and anti-Ubiquitin antibodies. Expression of wild type protein does not cause ubiquitination (Figure 3I-J), whereas aggregates induced by P58S dVAP expression stain positively with anti-Ubiquitin antibodies (Figure 3K-L). As shown in Figure 3M, these aggregates are likely to contain insoluble P58S dVAP. The high molecular weight ladder seen in lane 8 (bracket) is consistent with ubiquitination. To confirm that P58S dVAP is ubiquitinated, we performed immunoprecipitation (IP) assays to isolate dVAP protein from flies expressing WT or P58S dVAP. We immunoblotted the IP products with anti-Ubiquitin antibodies. As shown in Figure 3N (bracket), the IP product from P58S dVAP, but not WT dVAP, is positive for Ubiquitin. In summary, P58S dVAP fails to be secreted, is ubiquitinated, and accumulates in cytoplasmic inclusions.

P58S dVAP accumulates in and disrupts the ER, and induces an unfolded protein response

VAPs are ER associated proteins that can form homodimers and heterodimers (Kaiser et al., 2005). To test whether P58S dVAP can recruit wild type dVAP to mutant inclusions, we first expressed WT FLAG-dVAP-HA and WT dVAP together in motor neurons. As shown in Figure 4 A-A″ and 4 C-C″, we find that WT FLAG-dVAP-HA is localized diffusely in the cytoplasm when it is co-expressed with WT dVAP.

When we overexpress WT FLAG-dVAP-HA and P58S dVAP together, we find that the tags are localized to inclusions (Figure 4B-4B″ and 4D-D″), indicating that WT dVAP is recruited into the inclusions. To determine if other ER associated proteins are present in these inclusions, we co-stained flies expressing P58S dVAP with anti-dVAP and anti-Boca, an ER marker (Culi and Mann, 2003). As shown in Figure 4F-F′, Boca is present in the inclusions. Similarly, Protein disulfide isomerase (PDI), another ER marker (Herpers and Rabouille, 2004), is also present in the inclusions (Figure 4H-H″). Transmission electron microscopy (TEM) of wing disc cells overexpressing WT or P58S dVAP shows that mutant dVAP causes abnormalities in the ER (Figure 4L-N). Flies expressing P58S dVAP exhibit clusters of aberrant electron-dense material (bracket in Figure 4N) that is continuous with the rough ER (arrow) in numerous cells. In summary, P58S dVAP recruits WT dVAP to cytosolic inclusions, alters the distribution of ER markers, and affects ER structure.

We next tested whether P58S dVAP induces an unfolded protein response (UPR), which has been documented in sporadic ALS as well as mutant *SOD1* transgenic animals (Atkin et al., 2006; Kikuchi et al., 2006). To evaluate the UPR, we assessed the expression of BiP/Hsc3, a member of the Hsp70 chaperone family and a primary sensor in the UPR (Elefant and Palter, 1999; Morris et al., 1997; Ryoo et al., 2007). As shown in Figure 4O-Q, adult brains overexpressing P58S dVAP exhibit significantly higher levels of Hsc3 (see Figure S3 for detail and western blot). These data suggest that P58S dVAP causes an UPR *in vivo*.

The phenotypic consequences of P58S dVAP overexpression

To assess the phenotypic consequences of P58S we compared overexpression of wild type and mutant protein in three different assays. First, presynaptic overexpression of the WT dVAP protein using the C155-GAL4 driver causes a significant increase in bouton number (Pennetta et al., 2002), whereas overexpression of the P58S mutant dVAP (Figure S4A) does not cause

a severe overgrowth phenotype. Second, we compared the ability of flies overexpressing mutant and wild type protein in a flight assay. Overexpression of WT dVAP significantly reduces flight ability, whereas overexpression of P58S dVAP causes only a mild phenotype (Figure S4B). These phenotypic differences are not due to differences in transgene expression (Figure S4C).

Finally, we performed ultrastructural studies of the indirect flight muscles. Wild type control animals (Figure 5A-B) display regular organization and uniform size of the myofibrils, and each myofibril (arrow) is smooth and surrounded by mitochondria (arrowhead). When the WT dVAP protein is expressed under the control of a neuronal driver (C155-GAL4) (Figure 5C-D), we find severe defects in 7% of the myofibrils. We do not observe these defects in wild type controls and flies expressing P58S dVAP (Figure 5G-H). In addition, the myofibrils are much more heterogeneous (mean of SD = 0.61 +/- 0.90, $P<0.01$ when compared to the control animals) in size when WT dVAP is overexpressed compared to when P58S is overexpressed (mean of SD = 0.33 +/- 0.70, $P<0.05$ when compared to the control animals; Figure 5E-F). These results indicate that overexpression of WT dVAP in neurons can cause muscle defects and that P58S dVAP does not replicate the phenotypes of overexpressed WT protein.

To determine the consequences of loss and overexpression of dVAP in synaptic transmission, we compared the electrophysiological properties of various animals. As shown in Figure S5 A and B, loss of function causes a moderate but significant increase in Excitatory Junctional Amplitude (EJP) amplitude and MiniEJP (mEJP) whereas overexpression of wild type or P58S induces a subtle reduction in EJP which is however not significant (Figure S5 C).

In summary, we have shown that the dVAP MSP domain is secreted and that WT dVAP overexpression can cause a cell non-autonomous defect. The P58S mutation prevents secretion, and potentially affects other functions such that overexpression of the mutant protein does not phenocopy that of wild type dVAP. P58S dVAP must retain some activity because overexpression of P58S dVAP in the nervous system (C155-GAL4) is able to rescue the lethality associated with the null mutations [data not shown and (Chai et al., 2008)]. Thus, P58S dVAP may be secreted at very low levels or secretion may not be required for all activities.

VAP MSP domains signal in an extracellular environment

The *C. elegans* genome contains a single VAP homolog, called F33D11.1 or VPR-1 (for VAP33-Related). However, 28 loci encode the sperm-specific MSPs, which are sperm-derived hormones that induce oocyte maturation and ovarian sheath contraction (Bottino et al., 2002; Yamamoto et al., 2006). When sperm and MSP are absent, oocyte maturation and sheath contraction rates are very slow, preventing oocyte loss (McCarter et al., 1999). Microinjecting purified, sperm-derived or recombinant MSP into the reproductive tract (Figure 6A) promotes oocyte maturation and sheath contraction (Miller et al., 2001). These responses are identical to those induced by wild type sperm and are not induced by other sperm proteins, endogenous bacterial proteins or several commercially available hormones (Corrigan et al., 2005; Miller et al., 2001).

The primary sequences of VAP MSP domains and MSPs are about 25% identical. If VAP MSP domains are secreted ligands for conserved receptors, they should be able to mimic the signaling activities of MSPs. To test this prediction, we microinjected purified, recombinant VPR-1 MSP domain into gonads lacking MSP and sperm (Figure 6A, B). As shown in Figure 6B, VPR-1 MSP stimulates a strong increase in oocyte maturation and sheath contraction rates over the same concentration range as MSP. Microinjecting dVAP and hVAP MSP domains also induces both responses (Figure 6B), suggesting that all MSP domains can signal through a common mechanism(s). The hVAP P56S mutant functions similarly to the wild type protein in this assay, indicating that this mutation does not affect signaling activity in the worm gonad.

We conclude that *C. elegans* MSP and VAP MSP domains have an evolutionarily conserved extracellular signaling activity.

VAPs and Eph receptors function in common genetic pathways

Previous studies indicate that sperm-derived MSPs binds to the VAB-1 Eph receptors and unidentified receptors expressed in oocytes and sheath cells (Govindan et al., 2006; Miller et al., 2003). We hypothesized that VAP MSP domains also regulate Eph receptors, which are widely expressed in fly, worm, and human nervous systems (George et al., 1998; Palmer and Klein, 2003). To test this hypothesis, we first sought to determine whether VAPs are required for the same *in vivo* processes as Eph receptors. Mutations in Eph receptors cause defects in cell and axon guidance during development (Klein, 2004). The *Drosophila* Eph receptor and its ligand Ephrin are required for proper axon guidance of the mushroom body (MB) neurons. Eph receptor and Ephrin mutations cause loss of alpha-lobes (Boyle et al., 2006). We found that *dVAP* null mutants and double mutants (ΔVAP; ΔEph) lack alpha-lobes in late pupae and adult brains (Figure S6 B,D; data not shown). The data indicate that both dVAP and Eph receptors are required for alpha lobe formation.

Overexpression of dVAP in neurons causes muscle defects in flies, consistent with a signaling function (Figure 5A-D). Eph receptor mutants suppress the muscle phenotypes (variable diameter of the myofibrils and myofibrillar degeneration) induced by overexpressing dVAP (Figure S6A-E). Moreover, Ephrin is present on muscles (Figure S6E-H). These data strongly argue that the non-autonomous and toxic activity of overexpressed dVAP is mediated by Eph receptors. Other requirements for Eph receptor and Ephrin in flies have yet to be determined, as the existing mutants are likely partial loss of function mutations (Dearborn et al., 2002).

To examine the role of *vpr-1* in *C. elegans* development, we characterized a *vpr-1(tm1411)* null mutant (Figure 6C, D). Phenotypes associated with *vpr-1 (tm1411)* can be rescued by transgenic expression of a fosmid containing *vpr-1*. Mutations in the VAB-1 Eph receptor or ephrin ligands cause incompletely penetrant and variably expressed phenotypes during development (Brenner, 1974; Chin-Sang et al., 1999; Chin-Sang et al., 2002; George et al., 1998; Wang et al., 1999; Zallen et al., 1999). We found that *vpr-1(tm1411)* mutants, similar to *vab-1* mutants, have incompletely penetrant and variably expressed defects. Loss of VPR-1, the ephrin EFN-2, or VAB-1 causes defects in distal tip cell (DTC) migration (Figure 6E and Figure S7A-C). The DTC is a gonadal leader cell whose migration path can be monitored using differential interference contrast (DIC) microscopy or the *lag-2::GFP* transgenic reporter, which expresses GFP in the DTC (Blelloch et al., 1999). Analysis of *vpr-1* and *vab-1* double mutants is consistent with these two genes acting in a common pathway during DTC migration (Figure 6E and Figure S7A).

VPR-1 and VAB-1 also function together to regulate the embryonic migrations of ventral hypodermal cells undergoing enclosure (Figure S7D,E) and amphid neurons (Figure 6F), whose final positions in adults can be visualized with dye DiI (Zallen et al., 1999). The amphids, as well as other head neurons, often lie too far posterior in *vpr-1(tm1411)* mutants compared to the wild type (Figure 6F,G). The amphids are sometimes positioned too far anterior in *vab-1 (dx31)* mutants (Figure 6F). Analysis of *vpr-1* and *vab-1* double mutants is consistent with *vpr-1* acting in *vab-1*-dependent and *vab-1*-independent mechanisms during embryogenesis (Figure 6F and S7D,E). Taken together, the data support the hypothesis that VAPs regulate Eph receptor signaling *in vivo*.

VAP MSP domains bind to Eph receptors

In the worm proximal gonad, the VAB-1 Eph receptor is expressed on oocyte and sheath cell surfaces (Figure 7A). VAB-1 and other MSP receptor sites can be visualized using fluorescein–

labeled MSP (MSP-FITC)(Miller et al., 2003). MSP-FITC is biologically active and binding can be out-competed with a 25-fold molar excess of unlabelled MSP (Figure 7B). To test whether VAP MSP domains can bind to cell surface receptors, we incubated ~200 nM FITC–labeled MSP domain conjugates with dissected gonads. VPR-1, hVAP, and dVAP MSP domains bind to oocyte and sheath cell plasma membranes in a pattern identical to MSP-FITC (Figure 7B, data not shown). Pre-incubation of worm gonads with a 25-fold molar excess of hVAP MSP domain out-competes hVAP-FITC binding, indicating that binding is specific. Moreover, MSP and hVAP likely bind to common receptors, as MSP-FITC binding can be out-competed with an excess of hVAP (Figure 7B). These results strongly support the hypothesis that VAP MSP domains bind to cell surface receptors.

To test whether VAP MSP domains can directly bind to the Eph receptor extracellular domain, we examined the interaction between VPR-1 MSP and VAB-1 Eph receptor. We produced a V5-tagged VAB-1 ectodomain (VAB-1 Ex V5) in HEK293T cells. We also expressed and purified a FLAG tagged VPR-1 MSP (VPR-1 MSP-FLAG) in bacterial cells and incubated the VPR-1 MSP-FLAG and VAB-1 Ex V5 proteins to assess binding by co-immunoprecipitation (co-IP). As shown in Figure 7C, anti-FLAG antibody co-immunoprecipitates the VAB-1 ectodomain (top panel) together with VPR-1 MSP (bottom panel). Furthermore, the anti-V5 antibody co-immunoprecipitates the VPR-1 MSP (Figure 7D, bottom panel) together with the VAB-1 ectodomain (Figure 7D, top panel). These data indicate that VPR-1 MSP is able to directly bind the VAB-1 ectodomain.

To examine the interaction between VAP MSP and Eph receptor in mammals, we produced a His and V5-tagged mouse EphA4 ectodomain (mEphA4Ex-V5His) and His tagged hVAP MSP (hVAPMSP-His). We incubated mEphA4Ex-V5His together with hVAPMSP-His proteins and performed co-IP assays with the V5 antibody. The V5 antibody is able to co-immunoprecipitate the hVAP MSP protein (Figure 7E, top panel) together with the EphA4 ectodomain (Figure 7E, bottom panel), suggesting that hVAP MSP binds to the EphA4 ectodomain directly.

Since VAP MSP can bind to the Eph receptor, VAP MSP might compete with Ephrins for Eph receptor binding. To perform competition experiments between hVAP MSP and Ephrin in mammalian cells, we used conditioned medium from HEK293T cells expressing secreted hVAP MSP or the EphA4 ligand, EphrinB2. We preincubated HEK293T cells expressing FLAG-tagged mouse EphA4 (FLAG-mEphA4) with conditioned medium containing hVAP MSP. Subsequently, we applied conditioned medium containing Fc-tagged mouse EphrinB2 (mEphrinB2-Fc) to the cells. After incubation, we retrieved mEphrinB2-Fc and EphA4 proteins complexes and immunoblotted with the anti-FLAG antibody. As shown in the top panel of Figure 7F and quantified in Figure 7G, hVAP MSP suppresses the binding of EphrinB2 to EphA4 in a dose dependent fashion. To confirm competition, we incubated mEphA4Ex-V5His and hVAPMSP-His proteins together with EphrinB2 protein. We again performed co-IP assays with V5 antibody (similar assay as in Figure 7E). Less hVAP MSP is recovered when EphrinB2 protein is increased in a dose dependent manner (Figure 7H, top panel), showing that EphrinB2 is able to out-compete hVAPB MSP for binding to EphA4 (quantified in Figure 7I). In summary, these data indicate that VAP MSP domains bind to the extracellular domain of Eph receptors and that this binding influences ephrin interactions.

Discussion

ALS is a disease caused by death of anterior horn motor neurons in the spinal cord and neurons in motor cortex, after decades of apparently normal development and function (Talbot and Ansorge, 2006). Familial and sporadic ALS cases as well as mouse models induced by overexpressing mutant *SOD1* indicate that all forms lead to intracellular cytoplasmic protein

inclusions containing ubiquitinated proteins (Basso et al., 2006; de Vrij et al., 2004; Moore et al., 2005). In flies expressing P58S dVAP, we find cytoplasmic inclusions and other key characteristics of ALS. First, P58S dVAP protein induces ubiqutinated inclusions. Second, the protein inclusions are associated with the ER and appear to be electron-dense ER expansions. Third, several key ER proteins colocalize with these inclusions. Finally, mutant dVAP induces an UPR. These data show at least three important parallels with ALS and *SOD1* mouse models: cytoplasmic inclusions, ubiquitination, and the UPR. The UPR-induced stress caused by P58S dVAP could eventually result in cellular damage or neuronal death (Chai et al., 2008).

Another feature associated with ALS is that the disease may have a cell non-autonomous component. We show that VAP MSP domains can be secreted, although not all cell types appear capable of secretion in flies (Figure 2). The VAP proteins, including the yeast homologue SCS2 have been proposed to be type II membrane proteins (Kagiwada et al., 1998). Since the proteins lack an N-terminal signal sequence, similar to MSP, secretion is likely to occur by an unconventional mechanism as observed for the *C. elegans* MSP proteins (Kosinski et al., 2005). In addition, the hVAP MSP domain is present in blood serum, a finding also supported by a large survey of serum proteins identified using mass spectrometry (Omenn et al., 2005). The MSP in serum may be able to bind to Eph receptors present on endothelial cells which regulate angiogenesis (Kuijper et al., 2007). Indeed, SOD1 mutants display defects in the tight junctions between endothelial cells and endothelial damage occurs prior to motorneuron degeneration (Zhang et al., 2008). Interestingly, Teuling et al. (2007) recently reported that VAPB is significantly decreased in the spinal cord of *SOD1* mutants and human patients with sporadic ALS. It is therefore possible that reduced signaling by the hVAP MSP domain is a mechanism responsible for some non-autonomous features associated with ALS pathogenesis.

Our results show that secreted MSP domains bind to Eph receptors on the surfaces of cells. Eph receptors also bind to ligands called ephrins (Pasquale, 2005). MSP domains function *in vivo* to antagonize ephrin signaling during oocyte maturation (Miller et al., 2003) and possibly amphid neuron migration. Our competition assays are consistent with MSP domains competing with ephrin for Eph receptor binding (Figure 7). In other processes, including worm DTC cell migration, ovarian sheath contraction, and fly mushroom body formation, MSP domains seem to be required for Eph receptor signaling (Miller et al., 2003). Hence, the relationship between MSP and ephrin ligands to Eph receptor signaling may depend on the developmental context, as previously observed for Ephrins and Eph receptors in mammals (Himanen et al., 2007). Multiple ephrins and Eph receptors including EphA4 and A7 are expressed throughout the adult nervous system and in skeletal muscle of vertebrate species (Iwamasa et al., 1999; Lai et al., 2001). Eph receptors regulate the survival of cultured spinal cord motor neurons (Magal et al., 1996), and influence proliferation and apoptosis in the adult mammalian CNS (Ricard et al., 2006). MSP dVAP may play a role in motor neuron survival or muscle function through interactions with Eph receptors.

Glutamate excitotoxicity is likely to play a role in the pathogenesis of ALS (Bruijn et al., 2004). Three lines of evidence suggest that VAP MSP domains might regulate glutamate receptor signaling. First, Eph receptors directly associate with NMDA-subtype glutamate receptors and regulate clustering in cultured neurons (Dalva et al., 2000). Second, loss of dVAP function or overexpression of P58S in flies is associated with increased glutamate receptor clustering and increased amplitudes of mEJPs at the NMJs (Chai et al., 2008; this work). Finally, MSP and the VAB-1 Eph receptor regulate NMDA receptor function during worm oocyte maturation (Corrigan et al., 2005).

We propose the following model for the pathogenesis of ALS8. The P56S hVAP protein accumulates in the ER, while the wild type protein is functional. In time, the aggregates become

more prominent, P56S hVAP becomes ubiquitinated, and functional wild type proteins become trapped in the inclusions. These protein inclusions initiate an UPR that eventually affects cell viability and lead to a decrease in MSP domain secretion. Impaired secretion decreases signaling by Eph receptors and other receptors. The mutant protein therefore causes two different defects: a cell autonomous defect in the ER that creates an UPR, and a cell non-autonomous defect resulting from reduced secretion of VAP MSP, which may function as an autocrine or paracrine signal. Both defects may synergize to produce the key features of ALS pathology. This model provides testable hypotheses and raises questions to be addressed in the future.

Experimental Procedures

Fly transgenes and strains

The PCR fragment of the *Drosophila* EST clone (LD30122) containing the *dVAP* coding sequence was subcloned into pUAST to generate UAS-dVAP. UAS-P58S dVAP was created by chimeric PCR with primers containing a P58S mutation. UAS-FLAG-dVAP-HA was created by chimeric PCR to add 3 FLAG tags and 2 HA tags at the N-terminus and C-terminus of the dVAP protein, respectively. UAS-hVAP was created by subcloning the coding sequence of hVAPB into the pUAST vector.

For the strains used in this study, see supplemental data.

Antibody generation and immunostaining

For dVAP antibody production and the list of the antibodies used in the study, see the supplemental data. Extracellular staining was performed as previously described (Seto and Bellen, 2006).

Protein chemistry

VAP MSP and Eph receptor binding assays—293T cells were transfected with the pcVAB-1Ex-V5His or pcEphA4Ex-V5His and incubated in OPTI-MEM (Invitrogen) for 2 days. The conditioned medium was collected and the Eph receptor extracellular domain proteins were purified on Ni beads. The bacterially expressed His-tagged VAP MSP proteins (FLAG-VPR-1MSP or hVAPMSP) were also purified with Ni beads. After desalting, Eph receptor extracellular domain protein and VAP MSP protein were incubated with each other in the binding buffer (50 mM Tris pH 8.0, 100 mM NaCl, 10% glycerol, 0.1% NP40, protease inhibitor cocktail) for 30 min at 25°C. The binding complexes were precipitated with anti-V5 (to pull down Eph receptor) or anti-FLAG (to pull down VPR-1MSP) antibody. The resulting precipitates were analyzed by western blotting with anti-V5, anti-FLAG or anti-His antibodies. To confirm the *in vitro* binding specificity between Eph A4 extracellular domain and hVAPMSP, the bacterially expressed His-tagged Ephrin B2 protein was incubated together with EphA4Ex-V5His and His-hVAPMSP. The binding complexes were immunoprecipitated with anti-V5 antibody and probed with anti-His antibody on western blot. Quantification: The western blot results of three independent experiments were scanned and analyzed by Image J. The binding affinity was indicated by the averaged ratio of pull down to input. The standard deviation is indicated by error bars.

For the constructs of the binding assays, protein fractionation, immunoprecipitation, serum purification, and the list of the antibodies, see supplemental data.

C. elegans experiments

Culture and genetic manipulations were carried out at 20°C as previously described, except that NA22 bacteria were used as the food source instead of the OP50 strain (Brenner, 1974).

N2 is the wild type strain. *vpr-1 (tm1411)* mutants were obtained from the Japanese Bioresource Project and backcrossed to the wild type five times. *tm1411* is a maternal effect sterile mutation. Microinjections, oocyte maturation and sheath contraction rate measurements, and FITC binding assays were performed as previously described (Corrigan et al., 2005). The amphid sensory neurons were labeled with the vital dye DiI (Zallen et al., 1998). DTC migration paths were visualized in L3 to young adult animals using the *lag-2::GFP* reporter, which expresses GFP in the DTC (Blelloch et al., 1999), DAPI staining, and DIC microscopy. For vpr-1 strain construction, marker scoring, rescue experiment, the genetic strains used, and 4D video microscopy, see supplemental data.

Supplementary Material

Refer to Web version on PubMed Central for supplementary material.

Acknowledgements

We thank the *Caenorhabditis* Genetics Center, the Japanese National Bioresource Project, D. Greenstein, G. Pennetta, S. Lev, H. Steller and H. Ryoo, J. Thomas, and A. Brand for reagents. We thank Y-C. He and J. Cao for technical assistance, and T. Lloyd, K. Schulze, A. Rajan, H. Andrews, D. Landis, and H.Y. Zoghbi for comments. Confocal microscopy was supported by the Mental Retardation and Developmental Disabilities Research Center. This work was supported by the American Cancer Society (RSG-06-151-01-DDC to M.A.M.). H.T. and K.M. have been supported by George and Ronya Kozmetsky. H.J.B. is an Investigator of the HHMI.

References

Amarilio R, Ramachandran S, Sabanay H, Lev S. Differential regulation of endoplasmic reticulum structure through VAP-Nir protein interaction. The Journal of biological chemistry 2005;280:5934–5944. [PubMed: 15545272]

Atkin JD, Farg MA, Turner BJ, Tomas D, Lysaght JA, Nunan J, Rembach A, Nagley P, Beart PM, Cheema SS, et al. Induction of the unfolded protein response in familial amyotrophic lateral sclerosis and association of protein-disulfide isomerase with superoxide dismutase 1. The Journal of biological chemistry 2006;281:30152–30165. [PubMed: 16847061]

Baker AM, Roberts TM, Stewart M. 2.6 A resolution crystal structure of helices of the motile major sperm protein (MSP) of Caenorhabditis elegans. J Mol Biol 2002;319:491–499. [PubMed: 12051923]

Basso M, Massignan T, Samengo G, Cheroni C, De Biasi S, Salmona M, Bendotti C, Bonetto V. Insoluble mutant SOD1 is partly oligoubiquitinated in amyotrophic lateral sclerosis mice. The Journal of biological chemistry 2006;281:33325–33335. [PubMed: 16943203]

Blelloch R, Anna-Arriola SS, Gao D, Li Y, Hodgkin J, Kimble J. The gon-1 gene is required for gonadal morphogenesis in Caenorhabditis elegans. Dev Biol 1999;216:382–393. [PubMed: 10588887]

Boillee S, Vande Velde C, Cleveland DW. ALS: a disease of motor neurons and their nonneuronal neighbors. Neuron 2006;52:39–59. [PubMed: 17015226]

Bottino D, Mogilner A, Roberts T, Stewart M, Oster G. How nematode sperm crawl. Journal of cell science 2002;115:367–384. [PubMed: 11839788]

Boyle M, Nighorn A, Thomas JB. Drosophila Eph receptor guides specific axon branches of mushroom body neurons. Development (Cambridge, England) 2006;133:1845–1854.

Brenner S. The genetics of Caenorhabditis elegans. Genetics 1974;77:71–94. [PubMed: 4366476]

Brickner JH, Walter P. Gene recruitment of the activated INO1 locus to the nuclear membrane. PLoS Biol 2004;2:e342. [PubMed: 15455074]

Bruijn LI, Miller TM, Cleveland DW. Unraveling the mechanisms involved in motor neuron degeneration in ALS. Annu Rev Neurosci 2004;27:723–749. [PubMed: 15217349]

Chai A, Withers J, Koh YH, Parry K, Bao H, Zhang B, Budnik V, Pennetta G. hVAPB, the causative gene of a heterogeneous group of motor neuron diseases in humans, is functionally interchangeable with its Drosophila homologue DVAP-33A at the Neuromuscular Junction. Hum Mol Genet 2008;17:266–280. [PubMed: 17947296]

Chin-Sang ID, George SE, Ding M, Moseley SL, Lynch AS, Chisholm AD. The ephrin VAB-2/EFN-1 functions in neuronal signaling to regulate epidermal morphogenesis in C. elegans. Cell 1999;99:781–790. [PubMed: 10619431]

Chin-Sang ID, Moseley SL, Ding M, Harrington RJ, George SE, Chisholm AD. The divergent C. elegans ephrin EFN-4 functions inembryonic morphogenesis in a pathway independent of the VAB-1 Eph receptor. Development (Cambridge, England) 2002;129:5499–5510.

Corrigan C, Subramanian R, Miller MA. Eph and NMDA receptors control Ca2+/calmodulin-dependent protein kinase II activation during C. elegans oocyte meiotic maturation. Development (Cambridge, England) 2005;132:5225–5237.

Culi J, Mann RS. Boca, an endoplasmic reticulum protein required for wingless signaling and trafficking of LDL receptor family members in Drosophila. Cell 2003;112:343–354. [PubMed: 12581524]

Dalva MB, Takasu MA, Lin MZ, Shamah SM, Hu L, Gale NW, Greenberg ME. EphB receptors interact with NMDA receptors and regulate excitatory synapse formation. Cell 2000;103:945–956. [PubMed: 11136979]

de Vrij FM, Fischer DF, van Leeuwen FW, Hol EM. Protein quality control in Alzheimer's disease by the ubiquitin proteasome system. Progress in neurobiology 2004;74:249–270. [PubMed: 15582222]

Dearborn R Jr, He Q, Kunes S, Dai Y. Eph receptor tyrosine kinase-mediated formation of a topographic map in the Drosophila visual system. J Neurosci 2002;22:1338–1349. [PubMed: 11850461]

Elefant F, Palter KB. Tissue-specific expression of dominant negative mutant Drosophila HSC70 causes developmental defects and lethality. Molecular biology of the cell 1999;10:2101–2117. [PubMed: 10397752]

George SE, Simokat K, Hardin J, Chisholm AD. The VAB-1 Eph receptor tyrosine kinase functions in neural and epithelial morphogenesis in C. elegans. Cell 1998;92:633–643. [PubMed: 9506518]

Govindan JA, Cheng H, Harris JE, Greenstein D. Galphao/i and Galphas signaling function in parallel with the MSP/Eph receptor to control meiotic diapause in C. elegans. Curr Biol 2006;16:1257–1268. [PubMed: 16824915]

Harris JE, Govindan JA, Yamamoto I, Schwartz J, Kaverina I, Greenstein D. Major sperm protein signaling promotes oocyte microtubule reorganization prior to fertilization in Caenorhabditis elegans. Dev Biol 2006;299:105–121. [PubMed: 16919258]

Herpers B, Rabouille C. mRNA localization and ER-based protein sorting mechanisms dictate the use of transitional endoplasmic reticulum-golgi units involved in gurken transport in Drosophila oocytes. Molecular biology of the cell 2004;15:5306–5317. [PubMed: 15385627]

Himanen JP, Saha N, Nikolov DB. Cell-cell signaling via Eph receptors and ephrins. Curr Opin Cell Biol. 2007

Iwamasa H, Ohta K, Yamada T, Ushijima K, Terasaki H, Tanaka H. Expression of Eph receptor tyrosine kinases and their ligands in chick embryonic motor neurons and hindlimb muscles. Dev Growth Differ 1999;41:685–698. [PubMed: 10646798]

Kagiwada S, Hosaka K, Murata M, Nikawa J, Takatsuki A. The Saccharomyces cerevisiae SCS2 gene product, a homolog of a synaptobrevin-associated protein, is an integral membrane protein of the endoplasmic reticulum and is required for inositol metabolism. J Bacteriol 1998;180:1700–1708. [PubMed: 9537365]

Kagiwada S, Zen R. Role of the yeast VAP homolog, Scs2p, in INO1 expression and phospholipid metabolism. J Biochem (Tokyo) 2003;133:515–522. [PubMed: 12761300]

Kaiser SE, Brickner JH, Reilein AR, Fenn TD, Walter P, Brunger AT. Structural basis of FFAT motif-mediated ER targeting. Structure 2005;13:1035–1045. [PubMed: 16004875]

Kikuchi H, Almer G, Yamashita S, Guegan C, Nagai M, Xu Z, Sosunov AA, McKhann GM 2nd, Przedborski S. Spinal cord endoplasmic reticulum stress associated with a microsomal accumulation of mutant superoxide dismutase-1 in an ALS model. Proceedings of the National Academy of Sciences of the United States of America 2006;103:6025–6030. [PubMed: 16595634]

Klein R. Eph/ephrin signaling in morphogenesis, neural development and plasticity. Curr Opin Cell Biol 2004;16:580–589. [PubMed: 15363810]

Kosinski M, McDonald K, Schwartz J, Yamamoto I, Greenstein D. C. elegans sperm bud vesicles to deliver a meiotic maturation signal to distant oocytes. Development (Cambridge, England) 2005;132:3357–3369.

Kuijper S, Turner CJ, Adams RH. Regulation of angiogenesis by Eph-ephrin interactions. Trends in cardiovascular medicine 2007;17:145–151. [PubMed: 17574121]

Lai KO, Ip FC, Cheung J, Fu AK, Ip NY. Expression of Eph receptors in skeletal muscle and their localization at the neuromuscular junction. Mol Cell Neurosci 2001;17:1034–1047. [PubMed: 11414792]

Loewen CJ, Levine TP. A highly conserved binding site in vesicle-associated membrane protein-associated protein (VAP) for the FFAT motif of lipid-binding proteins. The Journal of biological chemistry 2005;280:14097–14104. [PubMed: 15668246]

Magal E, Holash JA, Toso RJ, Chang D, Lindberg RA, Pasquale EB. B61, a ligand for the Eck receptor protein-tyrosine kinase, exhibits neurotrophic activity in cultures of rat spinal cord neurons. J Neurosci Res 1996;43:735–744. [PubMed: 8984203]

McCarter J, Bartlett B, Dang T, Schedl T. On the control of oocyte meiotic maturation and ovulation in Caenorhabditis elegans. Dev Biol 1999;205:111–128. [PubMed: 9882501]

Miller MA, Nguyen VQ, Lee MH, Kosinski M, Schedl T, Caprioli RM, Greenstein D. A sperm cytoskeletal protein that signals oocyte meiotic maturation and ovulation. Science (New York, NY 2001;291:2144–2147.

Miller MA, Ruest PJ, Kosinski M, Hanks SK, Greenstein D. An Eph receptor sperm-sensing control mechanism for oocyte meiotic maturation in Caenorhabditis elegans. Genes Dev 2003;17:187–200. [PubMed: 12533508]

Moore DJ, West AB, Dawson VL, Dawson TM. Molecular pathophysiology of Parkinson's disease. Annual review of neuroscience 2005;28:57–87.

Morris JA, Dorner AJ, Edwards CA, Hendershot LM, Kaufman RJ. Immunoglobulin binding protein (BiP) function is required to protect cells from endoplasmic reticulum stress but is not required for the secretion of selective proteins. The Journal of biological chemistry 1997;272:4327–4334. [PubMed: 9020152]

Nishimura AL, Mitne-Neto M, Silva HC, Richieri-Costa A, Middleton S, Cascio D, Kok F, Oliveira JR, Gillingwater T, Webb J, et al. A mutation in the vesicle-trafficking protein VAPB causes late-onset spinal muscular atrophy and amyotrophic lateral sclerosis. American journal of human genetics 2004;75:822–831. [PubMed: 15372378]

Nishimura Y, Hayashi M, Inada H, Tanaka T. Molecular cloning and characterization of mammalian homologues of vesicle-associated membrane protein-associated (VAMP-associated) proteins. Biochemical and biophysical research communications 1999;254:21–26. [PubMed: 9920726]

Omenn GS, States DJ, Adamski M, Blackwell TW, Menon R, Hermjakob H, Apweiler R, Haab BB, Simpson RJ, Eddes JS, et al. Overview of the HUPO Plasma Proteome Project: results from the pilot phase with 35 collaborating laboratories and multiple analytical groups, generating a core dataset of 3020 proteins and a publicly-available database. Proteomics 2005;5:3226–3245. [PubMed: 16104056]

Palmer A, Klein R. Multiple roles of ephrins in morphogenesis, neuronal networking, and brain function. Genes Dev 2003;17:1429–1450. [PubMed: 12815065]

Pasquale EB. Eph receptor signalling casts a wide net on cell behaviour. Nat Rev Mol Cell Biol 2005;6:462–475. [PubMed: 15928710]

Pennetta G, Hiesinger PR, Fabian-Fine R, Meinertzhagen IA, Bellen HJ. Drosophila VAP-33A directs bouton formation at neuromuscular junctions in a dosage-dependent manner. Neuron 2002;35:291–306. [PubMed: 12160747]

Perry RJ, Ridgway ND. Oxysterol-binding protein and vesicle-associated membrane protein-associated protein are required for sterol-dependent activation of the ceramide transport protein. Molecular biology of the cell 2006;17:2604–2616. [PubMed: 16571669]

Pesacreta TC, Byers TJ, Dubreuil R, Kiehart DP, Branton D. Drosophila spectrin: the membrane skeleton during embryogenesis. The Journal of cell biology 1989;108:1697–1709. [PubMed: 2497103]

Ricard J, Salinas J, Garcia L, Liebl DJ. EphrinB3 regulates cell proliferation and survival in adult neurogenesis. Mol Cell Neurosci 2006;31:713–722. [PubMed: 16483793]

Ryoo HD, Domingos PM, Kang MJ, Steller H. Unfolded protein response in a Drosophila model for retinal degeneration. The EMBO journal 2007;26:242–252. [PubMed: 17170705]

Seto ES, Bellen HJ. Internalization is required for proper Wingless signaling in Drosophila melanogaster. The Journal of cell biology 2006;173:95–106. [PubMed: 16606693]

Skehel PA, Fabian-Fine R, Kandel ER. Mouse VAP33 is associated with the endoplasmic reticulum and microtubules. Proceedings of the National Academy of Sciences of the United States of America 2000;97:1101–1106. [PubMed: 10655491]

Soussan L, Burakov D, Daniels MP, Toister-Achituv M, Porat A, Yarden Y, Elazar Z. ERG30, a VAP-33-related protein, functions in protein transport mediated by COPI vesicles. The Journal of cell biology 1999;146:301–311. [PubMed: 10427086]

Strigini M, Cohen SM. Wingless gradient formation in the Drosophila wing. Curr Biol 2000;10:293–300. [PubMed: 10744972]

Talbot K, Ansorge O. Recent advances in the genetics of amyotrophic lateral sclerosis and frontotemporal dementia: common pathways in neurodegenerative disease. Human molecular genetics 2006;15(Spec No 2):R182–187. [PubMed: 16987882]

Teuling E, Ahmed S, Haasdijk E, Demmers J, Steinmetz MO, Akhmanova A, Jaarsma D, Hoogenraad CC. Motor neuron disease-associated mutant vesicle-associated membrane protein-associated protein (VAP) B recruits wild-type VAPs into endoplasmic reticulum-derived tubular aggregates. J Neurosci 2007;27:9801–9815. [PubMed: 17804640]

Wang PY, Weng J, Anderson RG. OSBP is a cholesterol-regulated scaffolding protein in control of ERK 1/2 activation. Science (New York, NY 2005;307:1472–1476.

Wang X, Roy PJ, Holland SJ, Zhang LW, Culotti JG, Pawson T. Multiple ephrins control cell organization in C. elegans using kinase-dependent and -independent functions of the VAB-1 Eph receptor. Mol Cell 1999;4:903–913. [PubMed: 10635316]

Ward S, Burke DJ, Sulston JE, Coulson AR, Albertson DG, Ammons D, Klass M, Hogan E. Genomic organization of major sperm protein genes and pseudogenes in the nematode Caenorhabditis elegans. J Mol Biol 1988;199:1–13. [PubMed: 3351915]

Weir ML, Klip A, Trimble WS. Identification of a human homologue of the vesicle-associated membrane protein (VAMP)-associated protein of 33 kDa (VAP-33): a broadly expressed protein that binds to VAMP. Biochem J 1998;333(Pt 2):247–251. [PubMed: 9657962]

Whitten SJ, Miller MA. The role of gap junctions in Caenorhabditis elegans oocyte maturation and fertilization. Dev Biol 2007;301:432–446. [PubMed: 16982048]

Yamamoto I, Kosinski ME, Greenstein D. Start me up: cell signaling and the journey from oocyte to embryo in C. elegans. Dev Dyn 2006;235:571–585. [PubMed: 16372336]

Zallen JA, Kirch SA, Bargmann CI. Genes required for axon pathfinding and extension in the C. elegans nerve ring. Development (Cambridge, England) 1999;126:3679–3692.

Zallen JA, Yi BA, Bargmann CI. The conserved immunoglobulin superfamily member SAX-3/Robo directs multiple aspects of axon guidance in C. elegans. Cell 1998;92:217–227. [PubMed: 9458046]

Zhong Z, Deane R, Ali Z, Parisi M, Shapovalov Y, O'Banion MK, Stojanovic K, Sagare A, Boillee S, Cleveland DW, et al. ALS-causing SOD1 mutants generate vascular changes prior to motor neuron degeneration. Nature neuroscience 2008;11:420–422.

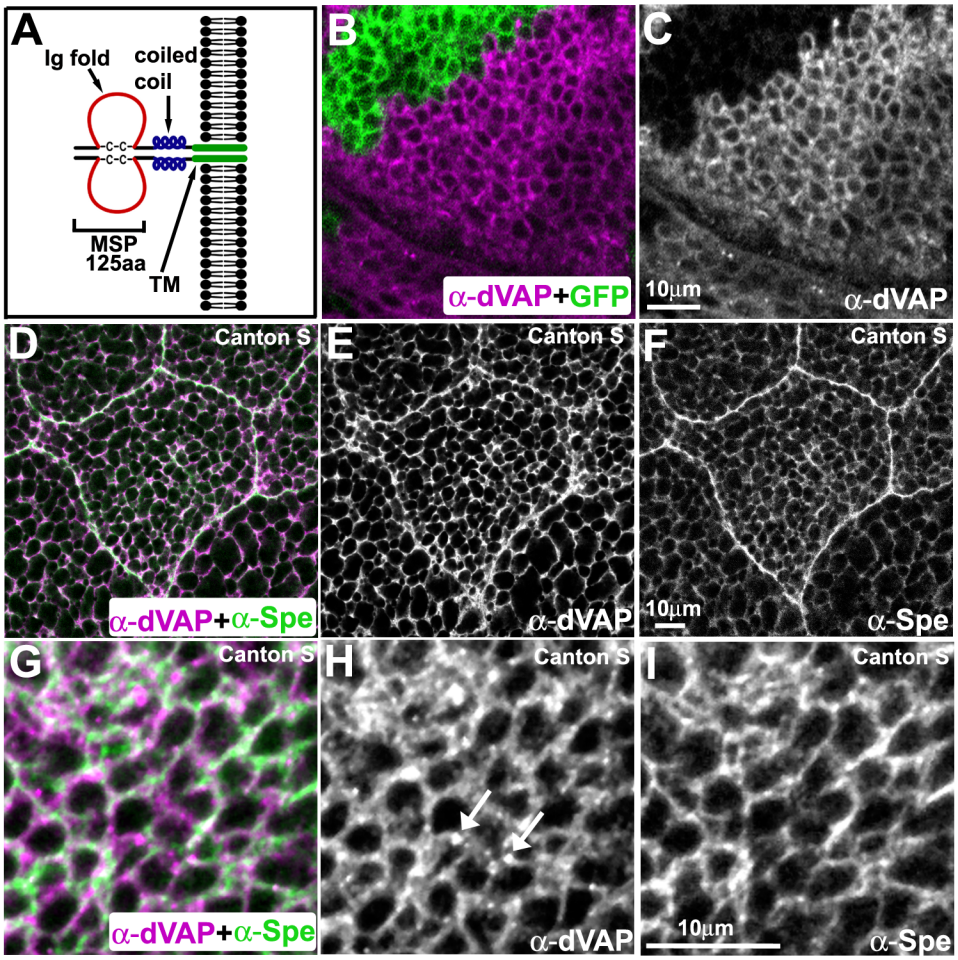

Figure 1. VAP localization

(A) The structure of VAPs. Note that VAPs form dimers.

(B-C) MARCM analysis showing the specificity of rabbit anti-dVAP antibody. A portion of the wing imaginal disc stained with anti-dVAP antibody (Rb92). GFP marks the mutant region (B). Single channel view of (B) showing only anti-dVAP (C).

(D-I) dVAP partially colocalizes with Spectrin. Salivary gland (D-F) and wing imaginal disc (G-I) of *Canton S* flies.

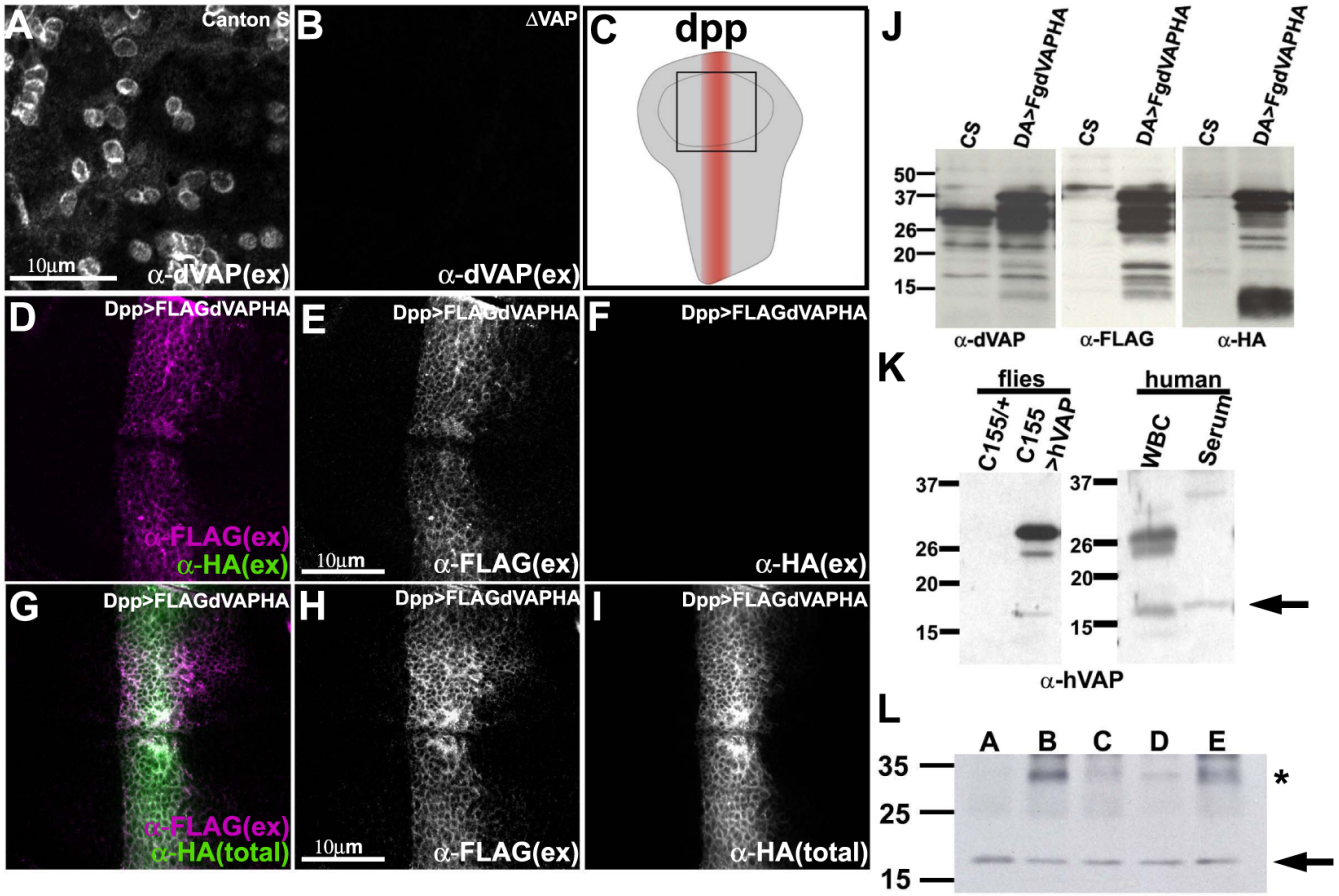

Figure 2. A portion of VAP is secreted

(A-B) dVAP in the wing disc is localized extracellularly. Staining of a wing pouch of Canton S (A) and *dVAP* null mutant (ΔVAP) (B) with anti-dVAP antibody (Rb92) without membrane permeabilization. Note that not all cells are decorated by dVAP.

(C) Pattern of expression of dpp-GAL4 in the wing imaginal disc. Anterior is to the *left*, ventral is to the *top*. The square in the center corresponds to Figure 2D-I.

(D-F) The N-terminal but not the C-terminal of dVAP is localized extracellularly. The wing disc expressing FLAG-dVAP-HA was co-stained with anti-FLAG and anti-HA without permeabilization.

(G-I) The N-terminal portion of dVAP is distributed more widely than the C-terminal portion. The wing disc expressing FLAG-dVAP-HA was stained with anti-FLAG extracellularly, and subsequently stained with anti-HA intracellularly (G). (total) intra- and extracellular staining. (ex) extracellular staining only.

(J) The N-terminal region of dVAP is cleaved from the full length protein. da-GAL4 was used to express FLAG-dVAP-HA ubiquitously. Extracts from Canton S (CS) and and flies expressing FLAG-dVAP-HA were immunoblotted with anti-dVAP (left panel), anti-HA (middle panel) and anti-FLAG (right panel).

(K) Truncated hVAP is expressed in human serum. Protein of wild type flies and those expressing hVAP were extracted and immunoblotted with anti-hVAP antibody (left panel). The extracts of human white blood cells and serum are immunoblotted with anti-hVAP antibody (right panel). Note that only the truncated hVAP protein is expressed in the serum (arrow in right panel).

(L) hVAP is expressed in human serum of five different individuals. The extracts of human serum were immunoblotted with anti-hVAP antibody. * indicates non-specific band (see Figure S1D).

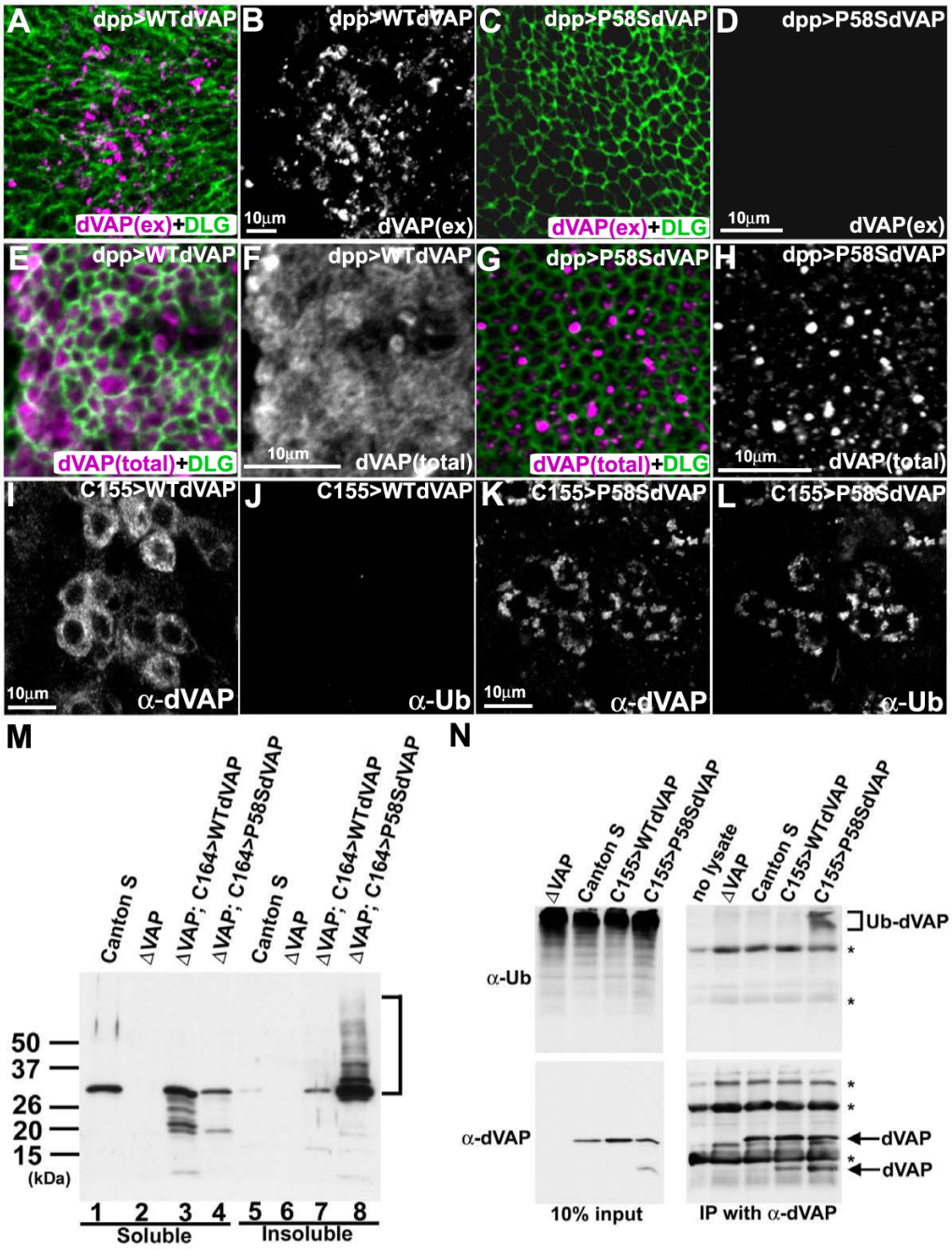

Figure 3. The P58S mutation leads to a failure to secrete dVAP and forms ubiquitinated inclusions

(A-D) The P58S mutation leads to a loss of the extracellular localization of dVAP. The wing discs expressing WT dVAP (A, B) and P58S dVAP (C, D) were stained using the anti-dVAP (magenta) extracellular staining protocol, and subsequently stained with anti-DLG (green) upon permeabilization.

(E-H) The P58S mutation causes dVAP protein to be localized as intracellular inclusions. Wing discs expressing WT dVAP (E, F) and P58S dVAP (G, H).

(I-L) Expression of P58S dVAP causes ubiquitin-containing inclusions. Neurons expressing WT dVAP (I, J) or P58S dVAP (K, L) were stained with anti-dVAP (I, K) and anti-Ubiquitin

(J, L). The laser intensity was adjusted for the signals of overexpressed proteins. Hence, endogenous expression of dVAP cannot be observed (Figure 3A-L).
(M) The P58S mutation causes detergent insoluble aggregates. Extracts of Canton S, null mutant (ΔVAP), and null mutant flies overexpressing WT or P58S dVAP were immunoblotted with anti-dVAP. Detergent soluble fractions (lane1-4); insoluble fractions (lane 5-8).
(N) P58S dVAP is ubiquitinated. Anti-dVAP (GP33) was used to immunoprecipitate dVAP from extracts of ΔVAP and flies expressing WT (C155>WTdVAP) or P58S dVAP (C155>P58SdVAP). Immunoblots of anti-Ubiqutin (right top panel) and anti-dVAP (right bottom panel). (bracket) ubiquitin positive high molecular weight products * non-specific signals.

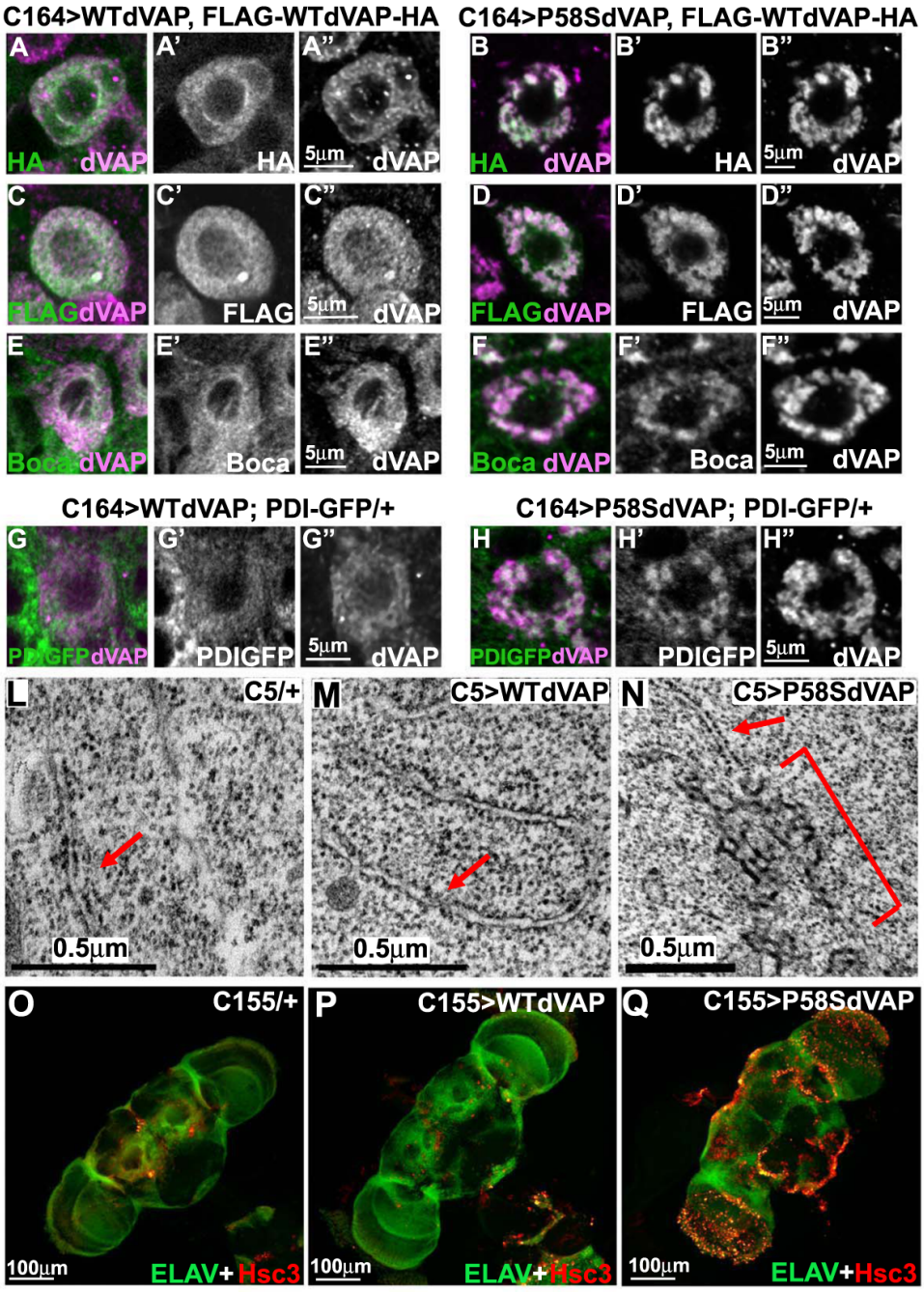

Figure 4. P58S dVAP protein accumulates in the ER, causes morphological changes in the ER, and induces an UPR

(A-D″) Single motorneurons expressing WT FLAG-dVAP-HA probed with HA or FLAG antibodies. WT dVAP (A-A″, C-C″) or P58S dVAP (B-B″, D-D″) and FLAG-WTdVAP-HA are expressed in motor neurons with the C164-GAL4 driver. Note that all motor neurons expressing P58S dVAP have protein aggregates.

(E-F″) Boca is localized diffusely in the cytoplasm in flies expressing WT dVAP. In contrast, Boca is localized in inclusions in flies expressing P58S dVAP.

(G-H″) PDI-GFP is localized diffusely in the cytoplasm when WT dVAP is co-expressed in PDI-GFP transgenic flies. In contrast, PDI-GFP is present in inclusions when P58S dVAP is expressed.

(L-N) TEM analysis of wing disc cells expressing WT or P58S dVAP with C5-GAL4, a wing pouch driver. Note that flies expressing P58S dVAP (N) contain clusters of aberrant electron-dense material (bracket) that is continuous with the rough ER (arrow). These clusters were commonly observed in C5>P58SdVAP (n=3 flies) and were never observed in wild type control cells (n=3 flies).

(O-Q) Overexpression of P58S dVAP causes an UPR. Anti-Hsc3 and anti-Elav costaining of adult brains of control flies (O), flies expressing WT dVAP (P) or P58S dVAP (Q).

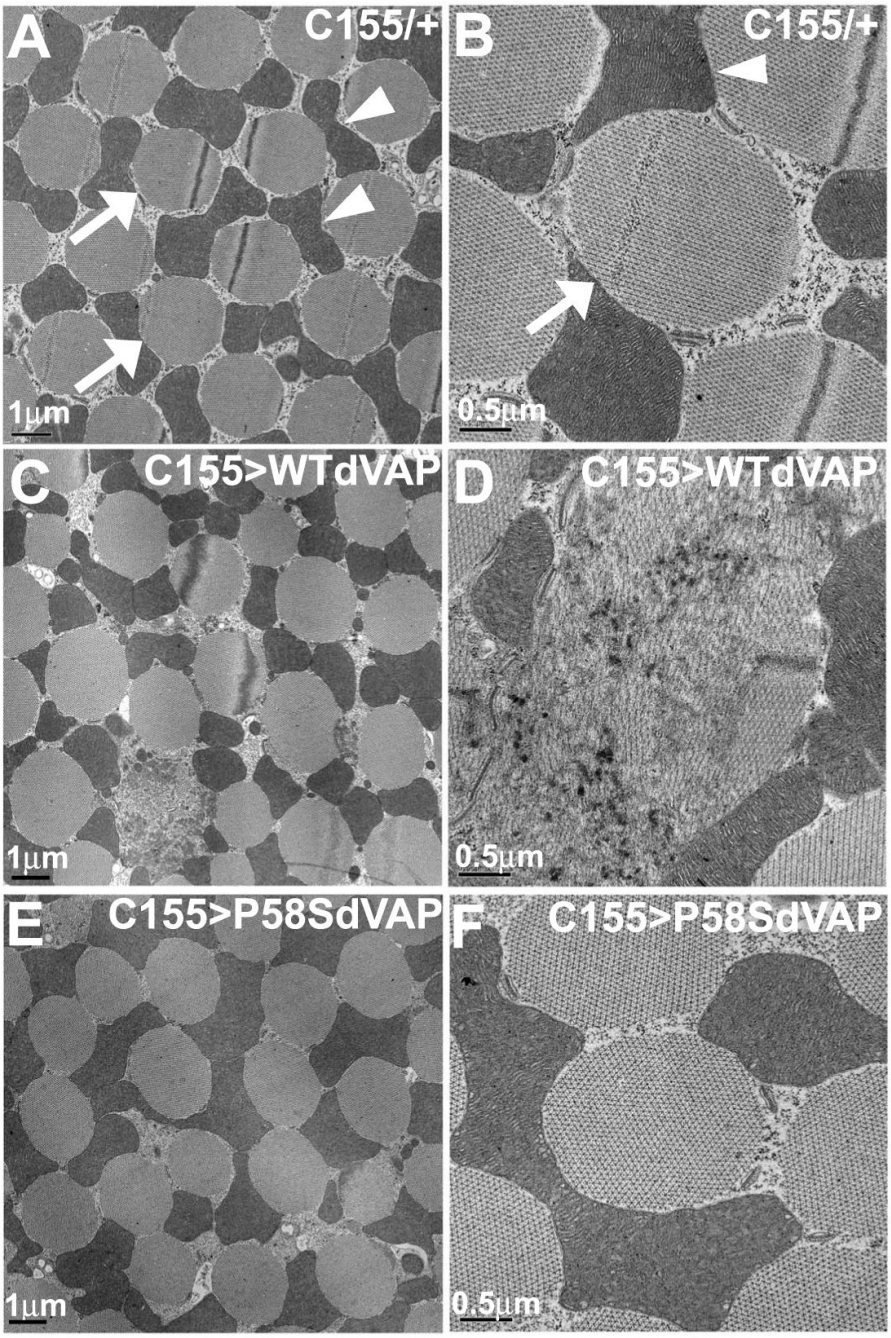

Figure 5. Overexpression of P58S dVAP does not phenocopy WT dVAP overexpression

TEM analysis of the dorsal ventral muscle (DVM) of flies overexpressing various dVAPs in neurons. Control animals (A-B), flies overexpressing neuronal WT dVAP (C-D) and P58S dVAP (E-F). Five animals, >30 muscles/animal were examined of each genotype.

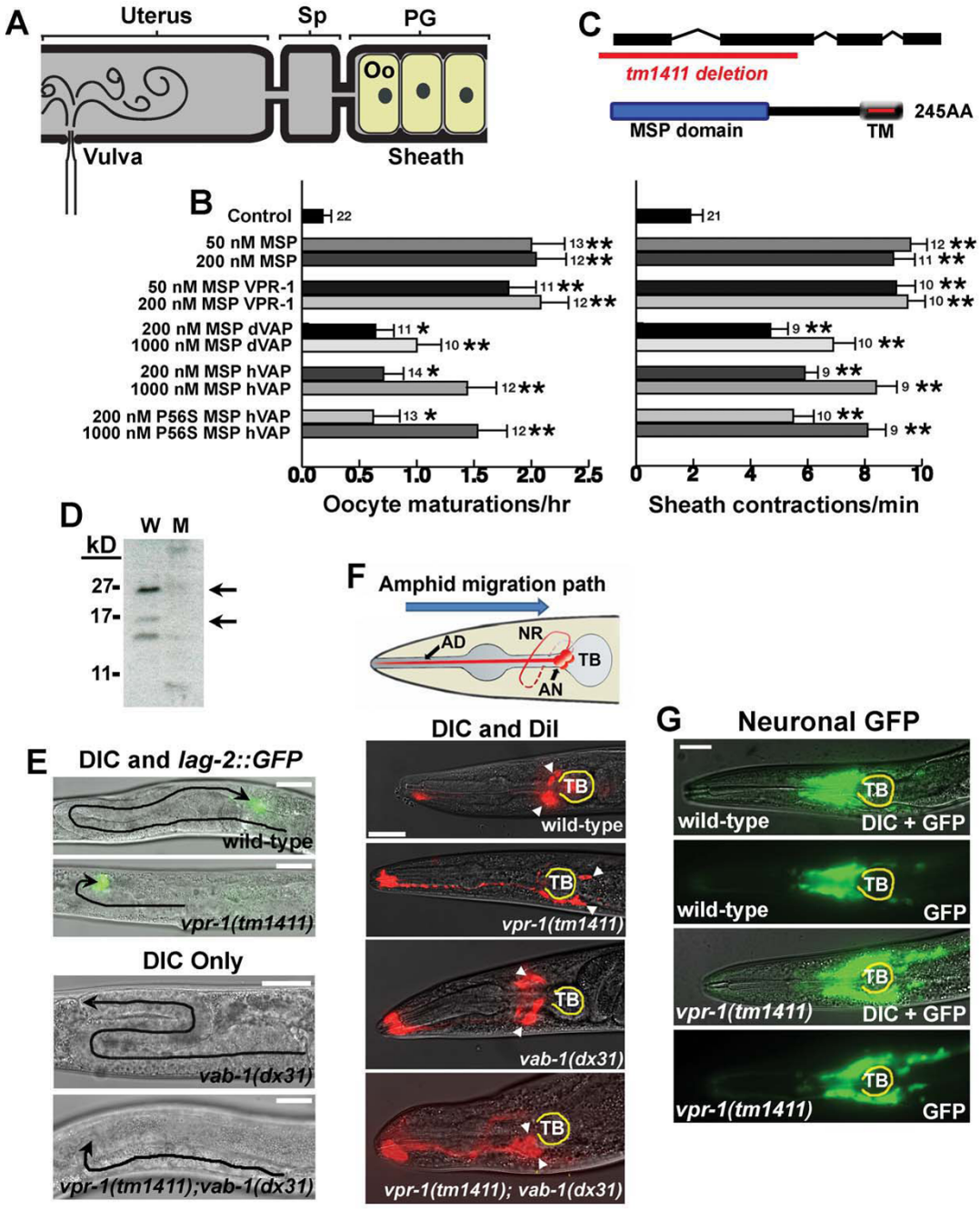

Figure 6. VAPs have extracellular signaling activity and act in common genetic pathways with Eph receptors

(A-B) VAP MSP domains have extracellular signaling activity. (A) Microinjection is used to test molecules for the ability to induce oocyte (Oo) maturation and sheath contraction in unmated *fog-2(q71)* females, which lack sperm. Injected solutions diffuse into the spermatheca (Sp) and proximal gonad (PG).

(B) Microinjections of purified, recombinant MSP domains are compared to a buffer-alone control injection. Additional negative controls are described in Miller et al. 2001, Miller et al. 2003, and Corrigan et al. 2005. Oocyte maturations per hour and basal sheath contractions per minute were scored. Number of gonads is to the right of SEM bars. *, $P < 0.01$; **, $P < 0.001$.

(C) VPR-1 encodes the sole VAP homolog in the *C. elegans* genome. The *tm1411* allele deletes the translational start site and the MSP domain.
(D) Western analysis of mixed stage wild type (W) and *vpr-1(tm1411)* mutant (M) worms using antibodies against *Drosophila* VAP (Rb 92).
(E) Distal Tip Cell (DTC) migration paths (black lines) in wild type and mutant hermaphrodites. *vpr-1(tm1411)* and *vab-1(dx31)* null mutants have incompletely penetrant and variably expressed defects in DTC migration (also see Fig. S7A). *vpr-1(tm1411); vab-1(dx31)* double mutants exhibit the same defects as *vpr-1(tm1411)* single mutants.
(F) Amphid neuron positions in wild type and mutant hermaphrodites. Amphid neurons (AN, diagram) migrate in an anterior to posterior direction during embryogenesis. Amphid cell body positions are shown by arrowheads. Loss of *vab-1* partially suppresses the posterior positioning defect of *vpr-1(tm1411)* mutants, although the double mutants have positioning and nerve ring (NR) defects not observed in either single mutant. The terminal bulb (TB) is outlined in yellow. Bars, 20 μm.
(G) Head neuron positions in wild type and *vpr-1(tm1411)* hermaphrodites. A pan-neuronal transgenic reporter shows that many head neurons are positioned too far posteriorly in *vpr-1 (tm1411)* mutants.

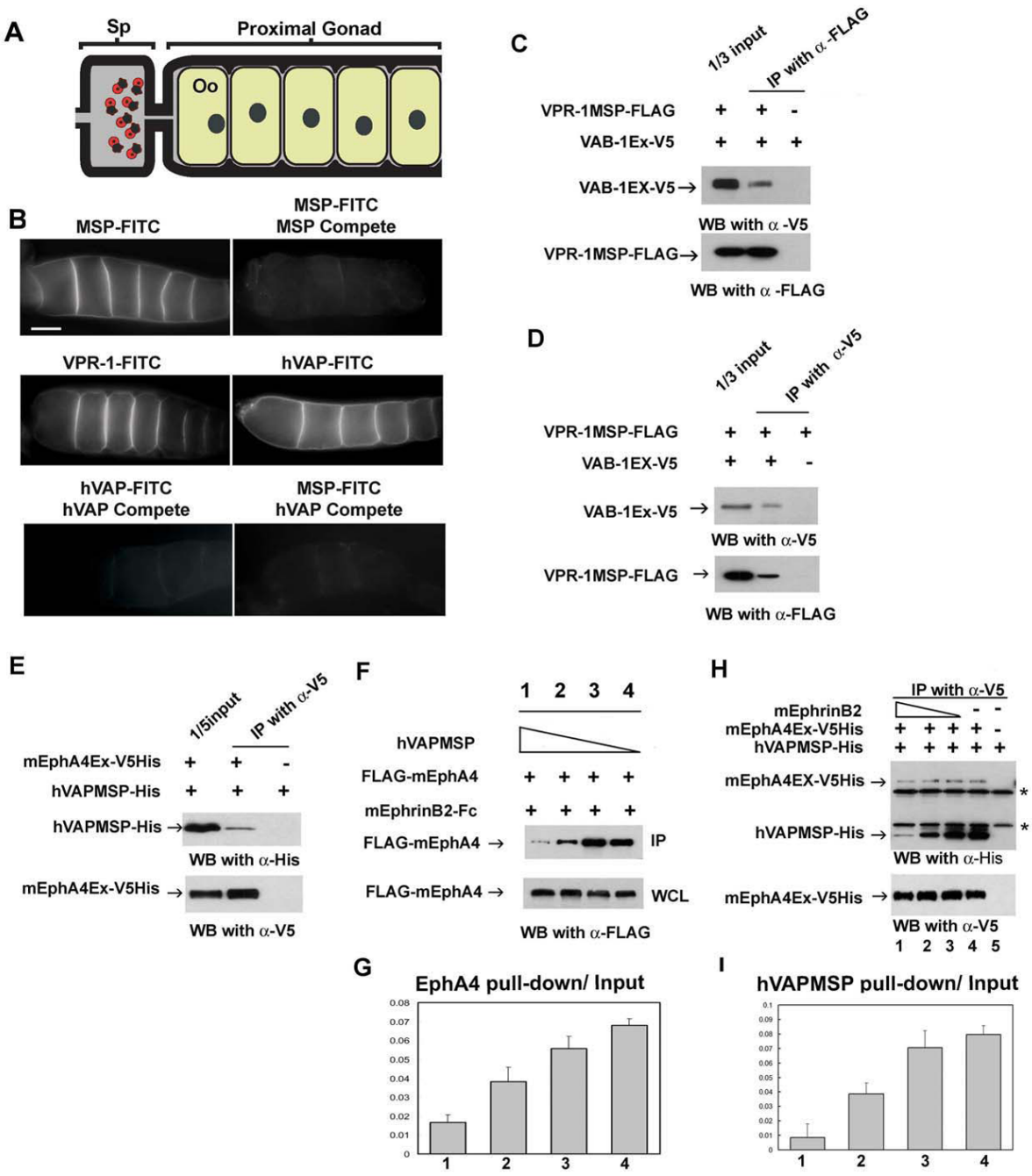

Figure 7. VAP MSP domains bind to Eph receptor extracellular domains

(A) Diagram of the *C. elegans* proximal gonad. MSP binds to receptors on the oocyte (Oo) and sheath cell surfaces in the proximal gonad (Miller et al. 2003; Corrigan et al. 2005).

(B) Receptor binding sites are visualized using FITC-conjugated MSP domains. FITC-conjugates are biological active in promoting oocyte maturation and sheath contraction (Miller et al. 2003; data not shown). Compete includes a 25-fold molar excess of unlabelled protein. Bar, 20 μm.

(C, D) VPR-1 MSP domain can bind to VAB-1 Eph receptor. Purified FLAG-tagged VPR-1 MSP (VPR-1MSP-FLAG) and V5 tagged VAB-1 ECT domain (VAB-1 Ex-V5) were co-immunoprecipitated using FLAG antibody (C) and V5 antibody (D). IP, immunoprecipitation.

(E) His- and V5- tagged mouse EphA4 ectodomain (mEphA4Ex-V5His) and a His tagged hVAPB MSP (hVAPMSP-His) co-immunoprecipitate using anti-V5 antibody.
(F) Conditioned medium containing hVAPMSP disrupts the interaction between mouse EphrinB2 (mEphrinB2) and EphA4. WCL: whole cell lysates.
(G) Quantification of the fraction of IP of (F). Lanes 1 to 4 correspond to the lanes in Figure 7F.
(H) Ephrin B2 competes with hVAPB MSP for binding of EphA4 in a dose dependent manner. As decreasing amounts of EphrinB2 are added, increasing amounts of hVAP MSP are pulled down by mEphA4Ex-V5 His. Note that EphrinB2-His cannot be detected in the top panel because it has a similar molecular weight to the IgG light chain. * shows non-specific heavy and light chains of IgG.
(I) The quantification of the fraction of IP of (H). The lanes correspond to the lanes 1 to 4 in Figure 7H.